



Published in final edited form as:

Int J Mycobacteriol. 2016 December ; 5(4): 426–436. doi:10.1016/j.ijmyco.2016.06.018.

Inhibition of apoptosis by Rv2456c through Nuclear factor- κ B extends the survival of *Mycobacterium tuberculosis*

Kristen L. Jurcic Smith^{a,b} and Sunhee Lee^{a,b,c,*}

^aHuman Vaccine Institute, Duke University School of Medicine, Durham, NC, USA

^bDepartment of Molecular Genetics and Microbiology, Duke University School of Medicine, Durham, NC, USA

^cDepartment of Pathology, Duke University School of Medicine, Durham, NC, USA

Abstract

Mycobacterium tuberculosis, the causative agent of tuberculosis, is an intracellular pathogen with several survival mechanisms aimed at subverting the host immune system. Apoptosis has been shown to be mycobactericidal, to activate CD8⁺ T cells, and to be modulated by mycobacterial proteins. Since few mycobacterial proteins have so far been directly implicated in the interactions between *M. tuberculosis* and host cell apoptosis, we screened *M. tuberculosis* H37Rv transposon mutants to identify mutants that fail to inhibit cell death (FID). One of these FID mutants, FID19, had a transposon insertion in Rv2456c and is important for survival in host cells. The lack of the protein resulted in enhanced caspase-3 mediated apoptosis, which is probably due to an inability to activate nuclear factor- κ B. Additionally, FID19 infection enhanced polyfunctional CD8⁺ T cells and induced a higher frequency of interferon- γ secreting immune cells in a murine model. Taken together, our data suggest that Rv2456c is important for the survival of H37Rv by subduing the innate and ultimately adaptive immune responses of its host by preventing apoptosis of the infected cell. Better understanding of the host-mycobacterial interactions may be beneficial to develop novel drug targets and engineer more efficacious vaccine strains against tuberculosis.

Keywords

Apoptosis; *Mycobacterium tuberculosis*; Tuberculosis; Vaccine

Introduction

Tuberculosis is a serious global health threat, infecting 9 million new individuals and causing 1.5 million deaths each year [1]. The prime etiological agent of this disease is *Mycobacterium tuberculosis*, an aerobic, acid-fast bacillus that dwells inside host cells after

This is an open access article under the CC BY-NC-ND license (<http://creativecommons.org/licenses/by-nc-nd/4.0/>).

*Corresponding author at: DUMC Box 103020, 1033 Global Health Research Building, 909 South LaSalle Street, Durham, NC 27710, USA. Sunhee.lee@duke.edu (S. Lee).

Conflicts of interest

The authors declare that the research was conducted in the absence of any commercial or financial relationships that could be construed as a potential conflict of interest.

infection [2,3]. The pathogen is transmitted via aerosolized particles from an actively infected individual [4], and it primarily resides inside host alveolar macrophages [5]. Once inside its targeted cell, the mycobacterium is able to modulate its surroundings in order to prevent immune detection and ensure survival.

As apoptosis is bactericidal to *M. tuberculosis*, it is not surprising that the bacterium has found ways to inhibit this pathway [6–11]. Cysteine proteases called caspases mediate apoptosis and are found in the cytoplasm until they are activated via cleavage at their active site [12]. Varieties of stimuli are able to induce cell death and can be found either internal or external to the cell. The Bcl-2 protein family regulates intrinsic apoptosis via their interactions with the mitochondrial membrane and can cause activation of caspase 9 [13]. Conversely, external stimuli such as tumor necrosis factor- α (TNF α) bind to death receptors on the exterior surface of the cell to initiate a cascade that activates caspase 8 [14]. These initiator caspases then activate caspase 3, which subsequently executes events that lead to apoptosis of the cell.

M. tuberculosis is able to block both the intrinsic and extrinsic apoptotic pathways. The bacterium reduces extrinsic apoptosis by preventing the secretion of Fas [6] and TNF α [8,15], as well as by interacting with host proteins [9]. Intrinsic apoptosis is abrogated through the upregulation of a prosurvival Bcl-2 protein, Mcl-1 [10]. Other genes have been identified as being important in the inhibition of apoptosis [8,16], but the specific mechanisms remain elusive. Thus, additional study in this area could uncover novel ways to prevent the survival of *M. tuberculosis* within host cells. It was reported that inhibition of apoptosis by *M. tuberculosis* could prevent cross presentation and activation of CD8⁺ T cells [17,18], minimizing the cytotoxic adaptive immune response. By identifying how the bacterium is able to subvert host immune responses in macrophages, it may be possible to engineer a nonpathogenic strain of *M. tuberculosis* that enhances immune responses for use as a vaccine. This is urgently needed, as there is no efficacious vaccine against tuberculosis [19,20].

To identify genes that are important in the inhibition of apoptosis, a transposon mutant library of *M. tuberculosis* H37Rv was generated and screened for mutants unable to inhibit cell death. Mutants were further screened for heightened immunogenicity in comparison to the parental strain. Based on its failure to inhibit apoptosis and to induce an immune response, fails to inhibit cell death mutant 19 (FID19), a transposon insertion in Rv2456c, was selected for further study. Our studies aimed to determine how this protein inhibits apoptosis in the wild type bacterium, if it is important for survival, and if a mutant lacking this protein has enhanced immunogenicity *in vivo*.

Materials and methods

Bacterial strains and culture conditions

M. tuberculosis H37Rv was obtained through the National Institute of Health Biodefense and Emerging Infectious Research Resources Repository (BIH-*M. tuberculosis*, strains H37Rv and NR-123). An arrayed transposon library containing 9400 mutants was generated through Mariner transposon mutagenesis as described previously [21]. The flanking

genomic region of the transposon insertion site was sequenced and the disrupted gene was complemented by either a plasmid expressing the single target gene with its promoter or a cosmid encoding the gene. A cosmid used for the complementation was generously provided by Dr. William R. Jacobs, Jr. (Albert Einstein School of Medicine, New York, NY, USA). To reduce variability between experiments, freshly frozen bacterial stocks were used for infection. To prepare the stocks, bacteria were grown until they reached an optical density between 0.6 and 0.8. At this point, the cells were washed twice in phosphate buffered saline (PBS; Gibco, Invitrogen, Carlsbad, CA) with 0.05% tyloxapol (Sigma–Aldrich, Hamburg, Germany), passed through a sterile 40 µM filter, and finally through a sterile 20 µM filter. The optical density of the culture was then adjusted to 1.2, aliquoted into 1-mL vials, and quickly frozen using dry ice and ethanol. Mycobacterial liquid growth media consisted of Middlebrook 7H9 media (Difco, BD) supplemented with 0.5% glycerol (Sigma–Aldrich), 0.05% tyloxapol (Sigma–Aldrich), and 10% of a solution of oleic acid, albumin, dextrose, and catalase supplement (BD Diagnostics, Sparks, MD). For growth plates, Middlebrook 7H10 media was supplemented with the same components as above. Plates were grown in incubators at 37 °C with 5% CO₂ for 3 weeks or until colonies were visible.

Cell death assay

Human epithelial cells (A549: American Type Culture Collection, CCL-185) were infected at a multiplicity of infection (MOI) of 10 for 3 h with the arrayed transposon mutant library. After this time, cells were washed twice with PBS and fresh media containing 50 µg/mL of gentamycin was added. The experiment was allowed to continue for 3 days and the supernatant was assayed for lactate dehydrogenase (LDH; Cytotoxicity Detection Kit, Roche, Mannheim, Germany) to measure membrane damage and cell death. Mutants that induced significant LDH release were further tested for their ability to induce death in human monocyte-derived macrophages (THP-1: TIB-202, American Type Culture Collection, Manassas, VA). To measure cell death, THP-1 cells were differentiated with 10 ng/mL of phorbol myristate acetate overnight, washed twice with PBS, and then infected with an MOI of 10. THP-1 cells were infected as described above for 4 days after which cells were fixed with 4% formaldehyde and stained with terminal deoxynucleotidyl transferase 2'-deoxyuridine, 5'-triphosphate nick-end labeling (TUNEL) as described in the package insert (*In-situ* Cell Death Detection Kit; Roche). Cells were analyzed on a BD FACS Canto or BD LSRII (Becton Dickinson Biosciences, Rutherford, NJ) after staining. All flow cytometry data was analyzed using Flowjo software (TreeStar, Ashland, OR).

Measurement of pyroptosis induction

Small hairpin RNA (shRNA) knockdowns in *PYCARD* and *NLRP3* in THP-1 cells were generously provided by Dr. Jenny Ting (University of North Carolina, Chapel Hill, NC, USA) and are described elsewhere [22]. Cell death was measured by TUNEL staining and interleukin (IL)-1β secretion was measured by enzyme-linked immunosorbent assay (ELISA; eBiosciences, San Diego, USA).

Chemical inhibition of cell death

THP-1 cells were differentiated and infected. After 3 h of infection, the cells were washed and media containing 50 µg/mL of gentamycin was added for the duration of the

experiment. The cells were either treated with dimethyl sulfoxide (DMSO) (control), 50 μM of a caspase-3 inhibitor Z-DEVD-FMK (R&D Systems, Minneapolis, MN) or 50 μM of a pan-caspase inhibitor Z-VAD-FMK (R&D Systems). After 3 days of infection, apoptosis was measured via TUNEL staining.

Western blotting

Cells were washed twice with PBS and lysed via radioimmunoprecipitation assay buffer (Sigma–Aldrich) containing protease and phosphatase inhibitor cocktails (Sigma–Aldrich) for 10 min on ice. Protein samples originating in the Biosafety Level 3 (BSL3) laboratory were filtered through 0.22 μm SpinX columns to remove bacteria. Samples were stored at $-80\text{ }^{\circ}\text{C}$ until needed. Proteins were separated on MiniProtean precast polyacrylamide gels (Bio-Rad, Hercules, CA) and were transferred onto polyvinylidene fluoride membranes (Bio-Rad). Membranes were blocked in 5% Tris-buffered saline with Tween20 (TBST Sigma–Aldrich) for either 1 h at room temperature or overnight at $4\text{ }^{\circ}\text{C}$. Primary antibodies were added at a 1:1,000 dilution in 5% bovine serum albumin (Sigma–Aldrich) in TBST at $4\text{ }^{\circ}\text{C}$ overnight (β -actin; Genscript, Piscataway, NJ; myeloid cell leukemia-1 [Mcl-1], nuclear factor [NF]- κB ; Cell Signaling Technology, Boston, MA). The membranes were then washed with TBST three times for 10 min each, and secondary antibodies (antimouse horseradish peroxidase; Genscript; antirabbit horseradish peroxidase; Cell Signaling Technology) were added at a dilution of 1:5000 for 1 h at room temperature in 5% bovine serum albumin in TBST. Membranes were again washed three times, and Lumi-Light Western Blotting Substrate (Roche) was used for the detection of proteins. ImageJ software program (US National Institutes of Health, Bethesda) was used for densitometry analysis and ratios were utilized to control for differences in loading.

Bacterial survival assays

For assessing *in vitro* survival of H37Rv and FID19, THP-1 cells were infected at an MOI of 10 as previously described. At indicated time points, cells were washed twice with PBS, and 0.1% Triton X-100 (Sigma–Aldrich) was added to each well for 10 min. At the end of the lysis period, the homogenate was plated. For *in vivo* survival, C57BL/6J mice were infected via the retro-orbital intravenous route with 1×10^7 bacteria. After 3 weeks of infection, the spleens were aseptically removed, homogenized, and plated. Colony counts were performed 3 weeks after plating to measure colony forming units (CFU).

Measurement of NF- κB activation

THP-1 cells were infected at an MOI of 10 for 2 days and then nuclear extracts were harvested utilizing a nuclear extraction kit (Abcam, Cambridge, MA). The extracts were filtered and assayed using an NF- κB p50/p65 transcription factor assay kit (Abcam) that measures p50 and p65 activation. An inhibitor of kappa B, BAY11-7082, was used to prevent NF- κB activation. Briefly, THP-1 cells were infected at an MOI of 10. DMSO as a control or BAY11-7082 was added to the infected cells. At 3- and 4-days postinfection, the cells were harvested and TUNEL stained to determine the effect of blocking NF- κB on cell death. Data are presented as a ratio of BAY-treated cells over DMSO-control cells.

In vitro immunogenicity screening

Bone marrow from C57BL/6J mice (Stock 000664; Jackson Laboratory, Bar Harbor, ME, USA) was harvested from long bones, depleted of red blood cells, and differentiated for 6 days in Dulbecco's Modified Eagle Medium media supplemented with penicillin–streptomycin and L929-conditioned media (20%) as previously described [23]. All bone marrow differentiation media was tested to ensure that a population of CD11b-positive (>95%) bone marrow derived macrophages (BMDMs) was present after 6 days. On Day 6, BMDMs were plated into 96-well plates (5×10^4 cells/well). The following day, the cells were infected with mycobacterial strains expressing Ag85-SIIN or $1 \mu\text{g/mL}$ of SIINFEKL peptide (Anaspec, Fremont, CA) was added as a positive control. CD8⁺ T cells were purified from OT-1 mice (Stock 004175; Taconic Biosciences Inc., Germantown, NY) via a cell separation method (MACS columns; Miltenyi Biotec, Auburn, CA) and added at a ratio of 5:1 OT-1 CD8⁺ T cells to BMDMs after 3 h of bacterial infection. The supernatant was collected after 24 h postaddition of the T cells and assayed for IL-2 and IFN γ via ELISA.

In vivo immunogenicity

All *in vivo* experiments were performed in compliance with the Institutional Biosafety Committee in a BSL3 facility at the Regional Containment Laboratory at Duke University, Durham, NC, USA. All animal studies were performed in accordance with approval of the Duke University Yale University's Institutional Animal Care and Use Committee. C57BL/6 J mice were injected via a retro-orbital intravenous route with 1×10^7 bacteria. Each inoculum was plated to determine if the CFU of the initial bacterial burden was consistent between groups. Mice were sacrificed 3 weeks post injection. For intracellular cytokine staining, the spleens were removed and mechanically homogenized in splenocyte media (RPMI-1640 media supplemented with 1% of both nonessential amino acids and penicillin–streptomycin) and lysed with ACK lysis buffer (Sigma–Aldrich). The cells were counted with a Moxi cell counter (Orflo, Hailey, ID) and plated at 2×10^6 cells. For each mouse, the samples were either left untreated or stimulated with Ag85 (Genscript; $10 \mu\text{g/mL}$), Tb10.4 (Genscript; $10 \mu\text{g/mL}$), or CD28 (BD; $2 \mu\text{g/mL}$) as a positive control. Golgistop (BD; $0.5 \mu\text{L/well}$) was added at the same time as the stimuli. All samples were performed in duplicate. Cells were stained for CD4⁺ (BD, San Jose, CA) and CD8⁺ (BD) surface markers and intracellular cytokines IL-2 (BD), TNF α (BD), and IFN γ (BD). Analysis was performed using a BD or L02. For Enzyme-Linked ImmunoSpot (ELISPOT) analysis, anti-IFN γ antibody (MabTech, Nacka Strand, Sweden) capture antibody was used. Mouse splenocytes were harvested and plated as described above. The cells were stimulated with Ag85 ($10 \mu\text{g/mL}$), Tb10.4 ($10 \mu\text{g/mL}$), PPD ($5 \mu\text{g/mL}$; Statens Serum Institute, Copenhagen, Denmark), concanavalin A (Sigma–Aldrich; $10 \mu\text{g/mL}$) as a positive control, or left cells untreated as an unstimulated control. A secondary antibody (MabTech), avidin peroxidase complex (Vectastain PK-6100; Vector Laboratories, Burlingame, CA), and 3-amino-9-ethylcarbazole substrate were used for detection. For removal from the BSL3, the plates were submerged in freshly made 1:128 Vesphene Ilse for a contact time of 10 min. This was then repeated, after which the plates were placed in bags and removed from the BSL3. The spots formed in the wells were counted on a C.T.L. Immunospot Analyzer (Cellular Technology Limited, Cleveland, OH) for determination of spot forming units (SFU). SFU

per well was used to calculate the total number of spot-producing cells per spleen (total SFU).

Statistical analysis

All statistical analysis was performed with Graphpad Prism software (San Diego, USA). A p value $< .05$ was considered significant. All data is presented as means \pm standard error of the means. Student t test were utilized for testing differences between the two groups and analysis of variance were employed for comparing more than two groups.

Results

Identification of cell death mutants of *M. tuberculosis*

A transposon mutant library of the common laboratory strain H37Rv was generated to identify genes that are important in the inhibition of cell death by *M. tuberculosis*. Mariner transposon mutagenesis was utilized for its random nature to insert into the genome between TA nucleotides [21]. The library consists of 9400 mutants, which should provide threefold coverage of the genome when essential genes are excluded. Human alveolar epithelial cells (A549) were used in the primary screen, as the cells have been previously used to evaluate mycobacterial infection-induced apoptosis [24–26]. Further, they do not require differentiation with phorbol 12-myristate 13-acetate like THP-1 cells, which made this high-throughput screen more manageable. It has been documented that if not engulfed by neighboring cells or in cell culture, where phagocytosis does not usually happen, the cells in the late stages of apoptosis present necrotic features due to the loss of cellular energy and plasma membrane integrity. This process is called “apoptotic necrosis” or “secondary necrosis” [27,28]. Thus, we analyzed the “apoptotic necrosis” of the A549 cells infected with an individual mutant using an LDH assay that is a reliable colorimetric method to quantitatively measure LDH released into the media from damaged cells. This method identifies mutants that have potentially undergone necrosis, pyroptosis, or apoptotic necrosis. In order to identify which mechanism of cell death occurred after infection with our mutants, secondary screening employing TUNEL staining (Fig. 1) was performed in THP-1 cells to identify transposon mutants exhibiting an apoptosis-inducing phenotype. Twenty-three out of 30 candidate transposon mutants from the screen consistently showed a significant increase in TUNEL positivity compared with the parental strain H37Rv. The interrupted genes, and therefore those likely to be important in the inhibition of cell death in wild-type H37Rv, were identified by sequencing the flanking regions of the transposon insertions. The mutants listed in Table 1 were confirmed to be proapoptotic and were numerically identified and termed FID mutants.

It is evident that *M. tuberculosis* has a multitude of mechanisms to inhibit cell death, as the functional groupings of the genes as annotated in Tuberculist (<http://tuberculist.epfl.ch/>) were diverse. Cell wall and cell wall processes were the most abundant proteins (34.78%) in this study, followed by those involved in intermediary metabolism and respiration (26.09%) and conserved hypotheticals (21.74%). There was dispersion of the transposon insertions throughout the genome, indicating acceptable mutagenesis coverage.

Rv2456c is important for inhibition of cell death and survival in host cells

FID19 was selected for further analysis based on its ability to enhance both cell death (Fig. 2B) and *in vitro* immunogenicity (Fig. 2D). Based on the sequence analysis, it was determined that a transposon was inserted between nucleotides 305 and 306 out of 1,257 base pairs of Rv2456c (Fig. 2A). The gene product is an integral membrane protein that is involved in solute transportation across the membrane, with the solute possibly being a sugar [29]. Complementation was achieved with expression of the full-length gene on a mycobacterial replicating plasmid (Fig. 2B). THP-1 cells were infected with H37Rv, FID19, or a complementation plasmid (FID19::pSL901) containing Rv2456c and TUNEL-positive cells were determined at 4 days postinfection. FID19 showed significantly higher TUNEL positivity compared with the parental wild type H37Rv strain. The complementing strain demonstrated the same level of apoptosis as the parental strain H37Rv (Fig. 2B). Survivability of a microbe within host cells is a measure of its virulence. In the human THP-1 cell model system, there was a trend, but not a statistically significant decrease in CFU between 1 day and 3 days post-FID19 infection (Fig. 2C).

Since FID19-infected cells undergo enhanced apoptosis (Fig. 2B), we would expect to see an increased ability of FID19 to induce a CD8⁺ T cell response [17,18]. To test this hypothesis, we utilized a variation of a previously described *in vitro* assay [30,31]. Briefly, BMDMs were infected with H37Rv or FID19 expressing SIINFEKL. To test this, OT-1 T cells that only recognized SIINFEKL were added to the infected BMDMs and T-cell activation was measured via IFN γ secretion. Indeed, levels of IFN γ secretion were significantly elevated in FID19–SIINFEKL infected cells when compared with H37Rv–SIIN cells (Fig. 2D). Low levels of IFN γ secretion can be detected in the absence of SIIN expression, specifically in the uninfected and H3Rv samples. Further, no statistically significant defect associated with FID19 growth in bacterial culture media was observed (Fig. 2E). These data suggest that Rv2456c is the gene that was disrupted through transposon mutagenesis and is responsible for the enhanced apoptotic phenotype and higher immunogenicity in the CD8⁺ T cell subset.

Apoptosis, not pyroptosis, mediated host cell death after FID19 infection

To elucidate how FID19-infected cells have enhanced cell death, cytokine secretion in infected THP-1 cells was examined. Secretion of TNF α and IL-1 β were elevated (Fig. 3A and B) in FID19 infected cells when compared with those infected with the parental strain H37Rv. TNF α , a known mediator of apoptosis, was secreted at a higher concentration in FID19 infected cells and decreased over time (Fig. 3A). H37Rv infection also induced TNF α secretion, but only at the 24-h time point, after which cytokine levels were similar to uninfected cells. Similarly, levels of an inflammatory cytokine, IL-1 β , were elevated as early as 24 h postinfection in FID19 infected cells and the concentration gradually increased over time, whereas levels in H37Rv infected cells remained constant (Fig. 3B).

The cytokine secretion profile after FID19 infection suggested that the mutant might also be inducing cell death through pyroptosis. Pyroptosis is an inflammatory form of cell death regulated by caspase-1 activation and results in the secretion of IL-1 β . To determine if pyroptosis played a role in death caused by FID19 infection, shRNA knockdown THP-1 cells were infected with either H37Rv or FID19. As previously reported [22], pyroptosis is

observed during H37Rv infection, as the percentage of TUNEL positive cells decreased when these proteins were absent. However, during FID19 infection the loss of *PYCARD* had no effect on cell death and the loss of *NLRP3* only slightly minimized cell death. These data indicated that pyroptosis mediated by these proteins does not play a role in cell death during FID19 infection (Fig. 3C). Additionally, since the knockdown cell lines are unable to secrete IL-1 β [22], it is likely that the cytokine is not responsible for the death of the host cells.

Chemical inhibitors of caspases were used to examine the role of apoptosis in cell death (Fig. 3D). Since caspase 3 is the main executioner caspase, an inhibitor was used to prevent its activation in THP-1 cells. A pan-caspase inhibitor was also employed to further measure the role of other caspases during infection. At 3 days postinfection, H37Rv infection in the DMSO-treated cells resulted in $12.5 \pm 2.0\%$ TUNEL positivity (Fig. 3D). Addition of the caspase-3 inhibitor or the pan-caspase inhibitor only slightly reduced cell death, measuring $8.3 \pm 1.7\%$ and $9.9 \pm 0.4\%$, respectively. By contrast, the percentage of cell death after FID19 infection in DMSO-treated cells was $51.6 \pm 2.2\%$ and the addition of the inhibitors significantly reduced cell death (caspase-3 inhibitor: 37.9 ± 2.4 , pan-caspase inhibitor: $25.3 \pm 0.1\%$, $p < .05$). These data show that cell death after FID19 infection is mediated by apoptosis and not pyroptosis.

Enhanced cell death after FID19 infection is a result of reduced NF- κ B activation

NF- κ B is a cellular survival pathway that can interact with the apoptotic pathway, and it has also been shown that *M. tuberculosis* can interfere with its regulation [32]. To determine if there were differences in NF- κ B activation after H37Rv and FID19 infection, expression of p50 and p65, two subunits of NF- κ B, was measured in nuclear extracts from infected THP-1 cells. There was a reduction in expression of both subunits 2-days postinfection in FID19-infected cells when compared with H37Rv or the complemented strain (Fig. 4A). When BAY11-7082, an inhibitor of inhibitory kappa B- α , was added to THP-1 cells infected with H37Rv or complemented FID19 there was an increase in cell death. However, there was no change when the inhibitor was added to cells infected with FID19 (Fig. 4B). To further confirm differences in NF- κ B activation, protein levels were assayed via western blot (Fig. 4C and D). FID19-infected cells had reduced protein expression of NF- κ B compared with H37Rv infected cells as early as 2-days postinfection. Additionally, FID19 infection also resulted in reduced levels of Mcl-1, an antiapoptotic protein of the Bcl-2 family (Fig. 4C and E). NF- κ B has been shown to regulate Mcl-1 [33,34]. Taken together, these results indicated that FID19 is unable to prevent apoptosis through activation of NF- κ B.

FID19 has enhanced in vivo immunogenicity in mouse studies

Proapoptotic mycobacterial mutants have been shown to induce enhanced immunity and are thus potential vaccine candidates [11,35]. In order to quantify the number of functional splenocytes capable of releasing IFN γ , we utilized ELI-SPOT analysis [36,37]. In the CD8⁺ T cell subset, FID19 infected mice had a mean of 303.6 ± 44.2 SFU/ 1×10^6 cells while H37Rv mice had a statistically lower mean of 139.8 ± 15.7 SFU/ 1×10^6 cells (Fig. 5A). There was also a statistical difference observed in the CD4⁺ T cell population when FID19 (360.5 ± 18.6 SFU) was compared to H37Rv (210.3 ± 25.0 SFU) infected mice. We determined the number of bacteria in the same harvested spleens that were utilized for

ELISPOT analysis. FID19-infected spleens had a significantly reduced bacterial burden compared to H37Rv infected spleens, even though the initial bacterial burden was comparable (Fig. 5B).

To further examine the ability of FID19 to induce an immunological response, mice were infected with FID19 or H37Rv. Polyfunctionality of T cells can be used as a measure of vaccine efficacy, as it has been shown to correlate with protection [38,39]. In our studies, FID19 infection increased both CD8⁺ and CD4⁺ polyfunctional T cell subsets when compared to H37Rv (Fig. 5C). Intracellular cytokine staining assays for IL-2, TNF α , and IFN γ production revealed that FID19 infection induced CD8⁺ T cells that secreted two cytokines at a higher percentage than H37Rv, 26% versus 20%, respectively. FID19 infection also induced 21% polyfunctional T cells, where H37Rv only induced 7%. In the CD4⁺ T cell subset, dual expression of cytokines was also increased after FID19 infection (30%) compared with H37Rv (26%). The same was also true when cells were secreting all three cytokines (FID19: 37%, H37Rv: 30%). These data suggest that FID19 induces a greater immune response during infection, which is likely due to enhanced antigen presentation through apoptosis induction. It also suggests that Rv2456c is important for the survival of *M. tuberculosis* within spleens.

Discussion

Our work has uncovered many genes that have not yet been associated with the inhibition of cell death by *M. tuberculosis* through the screening of a large transposon library. The genes identified are diverse in function, suggesting that this pathogen has a multitude of mechanisms to ensure its survival by preventing the death of its host cell. It is interesting to note that many of the proteins identified in this screen have unknown functions, and thus present an opportunity to learn more about the pathogenicity of *M. tuberculosis* (Table 1). It is unsurprising that the cell wall processes and metabolism and respiration functional groups were well represented, as these are important ways in which mycobacterium interact with their surroundings and modulate their growth to survive in host cells. Future studies of these genes will likely elucidate in vivo survival mechanisms of *M. tuberculosis*.

Our study did not identify genes previously found to have a role in cell death [6,7,9,11,15,40] caused by *M. tuberculosis*. There was overlap of a single gene, *Rv1436*, between the screen in this work and a screen performed by Danelishvili et al. [9]. The screens differed in both the cell types used as well as in the mechanism of detection. In our study, A549 cells were initially screened for membrane damage induced by 9400 transposon mutants and further confirmed through THP-1 cell infection followed by TUNEL staining (Fig. 1), whereas Danelishvili et al. [9] screened 5000 mutants in U937 and monitored for cellular detachment and ELISA confirmation. Additional genes that may interact or have homology with other genes identified in the literature. For example, *Rv1624c* (FID12) is a conserved hypothetical protein with some similarity to *M. tuberculosis* NuoK. This gene lies in an operon with NuoG, part of a nicotinamide adenine dinucleotide + hydrogen dehydrogenase found to aid in the inhibition of TNF α mediated apoptosis [8,15]. Additionally, *Rv1981c* (FID1) was identified in our screen, which is immediately upstream of *Rv1980c* (MPT64), and Wang et al. [32] recently established that MPT64 is able to

inhibit apoptosis through NF- κ B. Based on the discovery of the different functional groups of *M. tuberculosis* FID proteins, it seems evident that *M. tuberculosis* utilizes many mechanisms to inhibit death of host cells and our screen has uncovered novel genes important in that goal. These results also suggest that our screen was not comprehensive and that there are likely many more genes that play a role in cell death inhibition. Many factors could have prevented our identification of known genes, such as the time points utilized, the host cell type infected, or the lack of a transposon insertion in the gene. There also may be some genes that are essential for the growth of *M. tuberculosis* and thus will never be identified in a screen such as this.

FID19 was identified as a priority mutant because of its strong induction of cell death (Figs. 1 and 2B) and the enhanced *in vitro* immunogenicity data (Fig. 2D). Sequencing revealed that FID19 has a transposon insertion in *Rv2456c* (Fig. 2A), an integral membrane transport protein. Orthologs can be found in other pathogenic mycobacteria, including *Mycobacterium bovis*, *Mycobacterium avium*, *Mycobacterium ulcerans*, and *Mycobacterium marinum*, suggesting that it has a role in virulence. Complementation via a replicating plasmid (Fig. 2B) further confirmed the finding that the loss of *Rv2456c* was responsible for the enhanced cell death phenotype observed. The directionality of the transport and the identity of the substrate of the protein are not currently known. The molecule may play a direct or indirect role in the inhibition of apoptosis in wild-type *M. tuberculosis* through activation of NF- κ B (Fig. 4).

Rv2456c is the second gene in a predicted two-gene operon, with *Rv2457c* (*ClpX*) being the first gene (Fig. 2A). In *M. tuberculosis*, *ClpX* was found to be upregulated during infections in THP-1 cells [41]. *ClpX* is an essential gene [42] and can act as a chaperone molecule when alone or as a protease when associated with ClpP [43]. Without the presence of this protease, both *Listeria monocytogenes* and *Streptococcus pneumoniae* lose the ability to survive in macrophages and in mice, indicating a role in virulence [44–46]. The ClpXP protease was also found to regulate RecA in bacterial cell death by *Escherichia coli* [47]. Considering that this protein has been established in other systems as playing a role in virulence, future studies will determine the interaction between ClpX and *Rv2456c* and its effect on the survival of *M. tuberculosis*.

FID19 induces cell death through caspase-3 mediated apoptosis. This is supported by the fact that chemical inhibition of caspase 3 is able to reduce cell death (Fig. 3D), as well as the finding that FID19 induces greater levels of TNF α secretion in comparison to H37Rv (Fig. 3A). The cells infected with H37Rv were not impacted by the presence of the inhibitor (Fig. 3D), likely because the bacterium is already inhibiting the pathway [7,8]. Cytokine secretions are vital for cell signaling and are commonly assayed during cell death experimentation. The presence of the inflammatory cytokine IL-1 β could indicate the activation of pyroptosis (Fig. 3B), but others have shown that IL-1 β can be cleaved independently of caspase-1 activation during mycobacterial infection [22]. In shRNA knockdown cell lines, cell death induced by FID19 (Fig. 3C) was not impacted by the loss of *PYCARD*, an adaptor molecule important for the cleavage of IL-1 β . The loss of *NLRP3* does reduce TUNEL positivity, but this decrease is also observed in H37Rv infection. It is unclear if *NLRP3* plays a *PYCARD*-independent role in pyroptosis. IL-1 β is not important

in the induction of cell death by FID19, as the shRNA knockdown cell lines are unable to secrete this cytokine and are not impaired in their ability to undergo cell death (Fig. 3B).

Recently, Bai et al. [48] showed that there is reduced survival of *M. tuberculosis* when NF- κ B is inhibited. Another group showed that *Rv3402c* is important for the activation of NF- κ B [49]. Further, they showed that TNF α and IL-1 β were also increased, similar to what was observed after FID19 infection. Our studies have also shown that the expression of *Rv2456c* resulted in increased NF- κ B activation and a loss of Mcl-1 expression (Fig. 4C), which reduced host cell apoptosis.

Since increased apoptosis induced by *M. tuberculosis* is important to immunogenicity [11], this work sought to determine if any of the mutants were able to modulate the immune response differently than the parental strain H37Rv. Mouse models currently serve as the most common method of studying tuberculosis immunology [50–52]. FID19 consistently showed enhanced immunogenicity in both the CD8⁺ and CD4⁺ T cell subsets (Fig. 5). This is a promising result, as the lack of a CD8⁺ cell response is hypothesized to be a reason why the Bacillus Calmette–Guérin vaccine is inefficient at protecting against pulmonary tuberculosis. Unlike FID19, another proapoptotic mutant, *secA2*, showed enhanced priming of the adaptive immunity only in the CD8⁺ cell subset [11].

Conclusion

We have identified several genes important in the inhibition of cell death by *M. tuberculosis* have been identified by our study. A transposon mutant with a disruption in *Rv2456c*, known in this work as *FID19*, was found to cause infected cells to undergo enhanced cell death, which may be due to a failure to induce NF- κ B activation and a subsequent result of caspase-3 mediated apoptosis. Future studies will look at longer time points in mice to determine how long *FID19* is able to survive within mice. Additionally, since this mutant had enhanced CD4⁺ and CD8⁺ T cell responses when compared with H37Rv, we will further examine its efficacy as a potential vaccine candidate.

Acknowledgments

This work was supported by R21AI090434. We acknowledge the help of Holly Alley for help in the generation of the arrayed transposon mutant library, William R. Jacobs, Jr. (Albert Einstein College of Medicine) for the gift of a cosmid, and Jenny Ting (University of North Carolina) for THP-1 knockdown cell lines. Flow cytometry was performed in the Duke Human Vaccine Institute Research Flow Cytometry Shared Resource Facility and high containment work was performed in the Regional Biocontainment Laboratory at Duke University.

References

1. World Health Organization. Global Tuberculosis Report 2014. World Health Organization; Geneva: 2014.
2. Shinnick TM, Good RC. Mycobacterial taxonomy. Eur. J. Clin. Microbiol. Infect. Dis. 1994; 13:884–901. [PubMed: 7698114]
3. Pimm TP, Lucero CA, Falkinham JO 3rd. Health impacts of environmental mycobacteria. Clin. Microbiol. Rev. 2004; 17:98–106. [PubMed: 14726457]
4. Riley RL. Airborne infection. Am. J. Med. 1974; 57:466–475. [PubMed: 4212915]
5. Verrall AJ, Netea MG, Alisjahbana B, et al. Early clearance of *Mycobacterium tuberculosis*: a new frontier in prevention. Immunology. 2014; 141:506–513. [PubMed: 24754048]

6. Oddo M, Renno T, Attinger A, et al. Fas ligand-induced apoptosis of infected human macrophages reduces the viability of intracellular *Mycobacterium tuberculosis*. *J. Immunol.* 1998; 160:5448–5454. [PubMed: 9605147]
7. Balcewicz-Sablinska MK, Keane J, Kornfeld H, et al. Pathogenic *Mycobacterium tuberculosis* evades apoptosis of host macrophages by release of TNF-R2, resulting in inactivation of TNF-alpha. *J. Immunol.* 1998; 161:2636–2641. [PubMed: 9725266]
8. Velmurugan K, Chen B, Miller JL, et al. *Mycobacterium tuberculosis* nuoG is a virulence gene that inhibits apoptosis of infected host cells. *PLoS Pathog.* 2007; 3:e110. [PubMed: 17658950]
9. Danelishvili L, Yamazaki Y, Selker J, et al. Secreted *Mycobacterium tuberculosis* Rv3654c and Rv3655c proteins participate in the suppression of macrophage apoptosis. *PLoS One.* 2010; 5:e10474. [PubMed: 20454556]
10. Sly LM, Hingley-Wilson SM, Reiner NE, et al. Survival of *Mycobacterium tuberculosis* in host macrophages involves resistance to apoptosis dependent upon induction of antiapoptotic Bcl-2 family member Mcl-1. *J. Immunol.* 2003; 170:430–437. [PubMed: 12496428]
11. Hinchey J, Lee S, Jeon BY, et al. Enhanced priming of adaptive immunity by a proapoptotic mutant of *Mycobacterium tuberculosis*. *J. Clin. Invest.* 2007; 117:2279–2288. [PubMed: 17671656]
12. Shalini S, Dorstyn L, Dawar S, et al. Old, new and emerging functions of caspases. *Cell Death Differ.* 2015; 22:526–539. [PubMed: 25526085]
13. Czabotar PE, Lessene G, Strasser A, et al. Control of apoptosis by the BCL-2 protein family: implications for physiology and therapy. *Nat. Rev. Mol. Cell Biol.* 2014; 15:49–63. [PubMed: 24355989]
14. Gaur U, Aggarwal BB. Regulation of proliferation, survival and apoptosis by members of the TNF superfamily. *Biochem. Pharmacol.* 2003; 66:1403–1408. [PubMed: 14555214]
15. Miller JL, Velmurugan K, Cowan MJ, et al. The type I NADH dehydrogenase of *Mycobacterium tuberculosis* counters phagosomal NOX2 activity to inhibit TNF-alpha-mediated host cell apoptosis. *PLoS Pathog.* 2010; 6:e1000864. [PubMed: 20421951]
16. Jayakumar D, Jacobs WR Jr, Narayanan S. Protein kinase E of *Mycobacterium tuberculosis* has a role in the nitric oxide stress response and apoptosis in a human macrophage model of infection. *Cell Microbiol.* 2008; 10:365–374. [PubMed: 17892498]
17. Schaible UE, Winau F, Sieling PA, et al. Apoptosis facilitates antigen presentation to T lymphocytes through MHC-I and CD1 in tuberculosis. *Nat. Med.* 2003; 9:1039–1046. [PubMed: 12872166]
18. Winau F, Kaufmann SH, Schaible UE. Apoptosis paves the detour path for CD8 T cell activation against intracellular bacteria. *Cell Microbiol.* 2004; 6:599–607. [PubMed: 15186397]
19. Colditz GA, Brewer TF, Berkey CS, et al. Efficacy of BCG vaccine in the prevention of tuberculosis. Meta-analysis of the published literature. *J. Am. Med. Assoc.* 1994; 271:698–702.
20. Colditz GA, Berkey CS, Mosteller F, et al. The efficacy of bacillus Calmette-Guerin vaccination of newborns and infants in the prevention of tuberculosis: meta-analyses of the published literature. *Pediatrics.* 1995; 96:29–35. [PubMed: 7596718]
21. Rubin EJ, Akerley BJ, Novik VN, et al. *In vivo* transposition of mariner-based elements in enteric bacteria and mycobacteria. *Proc. Natl. Acad. Sci. U.S.A.* 1999; 96:1645–1650. [PubMed: 9990078]
22. McElvania Tekippe E, Allen IC, Hulseberg PD, et al. Granuloma formation and host defense in chronic *Mycobacterium tuberculosis* infection requires *PYCARD/ASC* but not NLRP3 or caspase-1. *PLoS One.* 2010; 5:e12320. [PubMed: 20808838]
23. Traver MK, Henry SC, Cantillana V, et al. Immunity-related GTPase M (IRGM) proteins influence the localization of guanylate-binding protein 2 (GBP2) by modulating macroautophagy. *J. Biol. Chem.* 2011; 286:30471–30480. [PubMed: 21757726]
24. Holla S, Ghorpade DS, Singh V, et al. *Mycobacterium bovis* BCG promotes tumor cell survival from tumor necrosis factor-alpha-induced apoptosis. *Mol. Cancer.* 2014; 13:210. [PubMed: 25208737]
25. Sohn H, Kim JS, Shin SJ, et al. Targeting of *Mycobacterium tuberculosis* heparin-binding hemagglutinin to mitochondria in macrophages. *PLoS Pathog.* 2011; 7:e1002435. [PubMed: 22174691]

26. Choi HH, Shin DM, Kang G, et al. Endoplasmic reticulum stress response is involved in *Mycobacterium tuberculosis* protein ESAT-6-mediated apoptosis. *FEBS Lett.* 2010; 584:2445–2454. [PubMed: 20416295]
27. Fink SL, Cookson BT. Apoptosis, pyroptosis, and necrosis: mechanistic description of dead and dying eukaryotic cells. *Infect. Immun.* 2005; 73:1907–1916. [PubMed: 15784530]
28. Majno G, Joris I. Apoptosis, oncosis, and necrosis. An overview of cell death. *Am. J. Pathol.* 1995; 146:3–15. [PubMed: 7856735]
29. Lew JM, Kapopoulou A, Jones LM, et al. TubercuList-10 years after. *Tuberculosis (Edinburgh Scotland).* 2011; 91:1–7.
30. Mazzaccaro RJ, Gedde M, Jensen ER, et al. Major histocompatibility class I presentation of soluble antigen facilitated by *Mycobacterium tuberculosis* infection. *Proc. Natl. Acad. Sci. U.S.A.* 1996; 93:11786–11791. [PubMed: 8876215]
31. Panas MW, Sixsmith JD, White K, et al. Gene deletions in *Mycobacterium bovis* BCG stimulate increased CD8⁺ T cell responses. *Infect. Immun.* 2014; 82:5317–5326. [PubMed: 25287928]
32. Wang Q, Liu S, Tang Y, et al. MPT64 protein from *Mycobacterium tuberculosis* inhibits apoptosis of macrophages through NF- κ B-miRNA21-Bcl-2 pathway. *PLoS One.* 2014; 9:e100949. [PubMed: 25000291]
33. Liu H, Yang J, Yuan Y, et al. Regulation of Mcl-1 by constitutive activation of NF- κ B contributes to cell viability in human esophageal squamous cell carcinoma cells. *BMC Cancer.* 2014; 14:98. [PubMed: 24529193]
34. Akgul C, Turner PC, White MR, et al. Functional analysis of the human MCL-1 gene. *Cell. Mol. Life Sci.* 2000; 57:684–691. [PubMed: 11130466]
35. Grode L, Seiler P, Baumann S, et al. Increased vaccine efficacy against tuberculosis of recombinant *Mycobacterium bovis* bacille Calmette–Guerin mutants that secrete listeriolysin. *J. Clin. Invest.* 2005; 115:2472–2479. [PubMed: 16110326]
36. Satti I, Meyer J, Harris SA, et al. Safety and immunogenicity of a candidate tuberculosis vaccine MVA85A delivered by aerosol in BCG-vaccinated healthy adults: a phase 1, double-blind, randomised controlled trial. *Lancet Infect. Dis.* 2014; 14:939–946. [PubMed: 25151225]
37. Lee J, Brehm MA, Greiner D, et al. Engrafted human cells generate adaptive immune responses to *Mycobacterium bovis* BCG infection in humanized mice. *BMC Immunol.* 2013; 14:53. [PubMed: 24313934]
38. Darrah PA, Patel DT, De Luca PM, et al. Multifunctional TH1 cells define a correlate of vaccine-mediated protection against *Leishmania major*. *Nat. Med.* 2007; 13:843–850. [PubMed: 17558415]
39. Forbes EK, Sander C, Ronan EO, et al. Multifunctional, high-level cytokine-producing Th1 cells in the lung, but not spleen, correlate with protection against *Mycobacterium tuberculosis* aerosol challenge in mice. *J. Immunol.* 2008; 181:4955–4964. [PubMed: 18802099]
40. Danelishvili L, Everman JL, McNamara MJ, et al. Inhibition of the plasma-membrane-associated serine protease cathepsin G by *Mycobacterium tuberculosis* Rv3364c suppresses caspase-1 and pyroptosis in macrophages. *Front. Microbiol.* 2011; 2:281. [PubMed: 22275911]
41. Dziedzic R, Kiran M, Plocinski P, et al. *Mycobacterium tuberculosis* ClpX interacts with FtsZ and interferes with FtsZ assembly. *PLoS One.* 2010; 5:e11058. [PubMed: 20625433]
42. Sassetti CM, Boyd DH, Rubin EJ. Genes required for mycobacterial growth defined by high density mutagenesis. *Mol. Microbiol.* 2003; 48:77–84. [PubMed: 12657046]
43. Frees D, Savijoki K, Varmanen P, et al. Clp ATPases and ClpP proteolytic complexes regulate vital biological processes in low GC, Gram-positive bacteria. *Mol. Microbiol.* 2007; 63:1285–1295. [PubMed: 17302811]
44. Gaillot O, Pellegrini E, Bregenholt S, et al. The ClpP serine protease is essential for the intracellular parasitism and virulence of *Listeria monocytogenes*. *Mol. Microbiol.* 2000; 35:1286–1294. [PubMed: 10760131]
45. Kwon HY, Ogunniyi AD, Choi MH, et al. The ClpP protease of *Streptococcus pneumoniae* modulates virulence gene expression and protects against fatal pneumococcal challenge. *Infect. Immun.* 2004; 72:5646–5653. [PubMed: 15385462]

46. Robertson GT, Ng WL, Foley J, et al. Global transcriptional analysis of clpP mutations of type 2 *Streptococcus pneumoniae* and their effects on physiology and virulence. *J. Bacteriol.* 2002; 184:3508–3520. [PubMed: 12057945]
47. Dwyer DJ, Camacho DM, Kohanski MA, et al. Antibiotic-induced bacterial cell death exhibits physiological and biochemical hallmarks of apoptosis. *Mol. Cell.* 2012; 46:561–572. [PubMed: 22633370]
48. Bai X, Feldman NE, Chmura K, et al. Inhibition of nuclear factor-kappa B activation decreases survival of *Mycobacterium tuberculosis* in human macrophages. *PLoS One.* 2013; 8:e61925. [PubMed: 23634218]
49. Li W, Zhao Q, Deng W, et al. *Mycobacterium tuberculosis* Rv3402c enhances mycobacterial survival within macrophages and modulates the host pro-inflammatory cytokines production via NF-kappa B/ERK/p38 signaling. *PLoS One.* 2014; 9:e94418. [PubMed: 24722253]
50. Korb DS, Schneider BE, Schaible UE. Innate immunity in tuberculosis: myths and truth. *Microbes Infect.* 2008; 10:995–1004. [PubMed: 18762264]
51. Aly S, Wagner K, Keller C, et al. Oxygen status of lung granulomas in *Mycobacterium tuberculosis*-infected mice. *J. Pathol.* 2006; 210:298–305. [PubMed: 17001607]
52. North RJ, Jung YJ. Immunity to tuberculosis. *Annu. Rev. Immunol.* 2004; 22:599–623. [PubMed: 15032590]

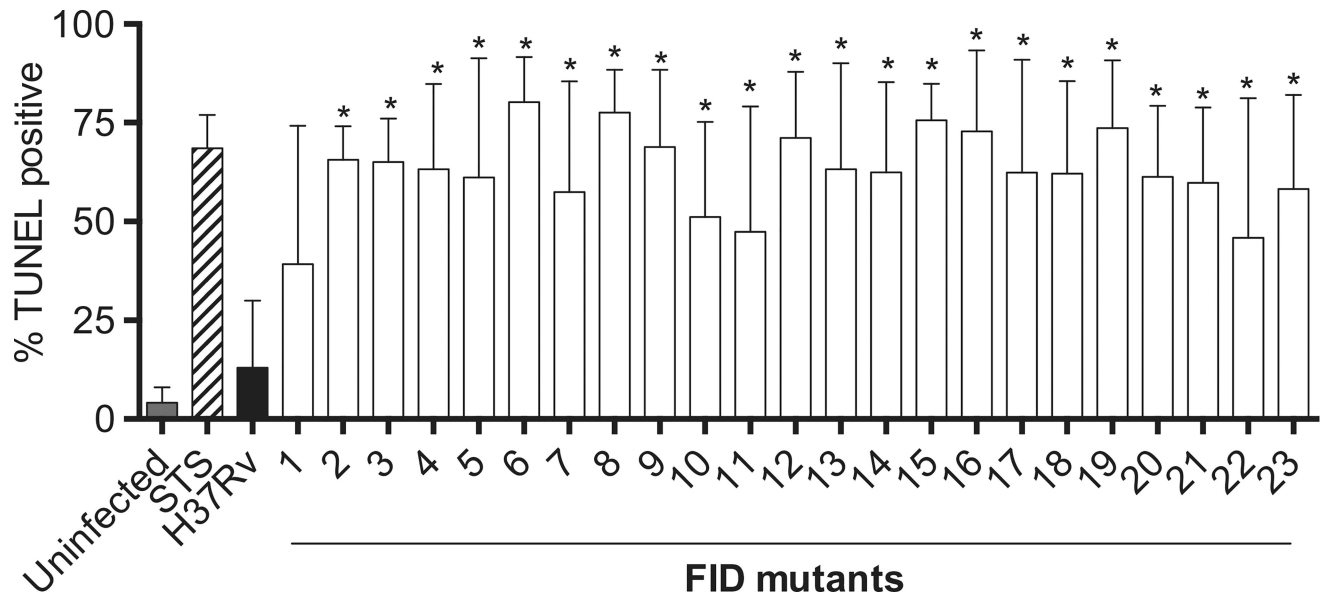


Fig. 1.

Cell death after *Mycobacterium tuberculosis* transposon mutant infection. THP-1 cells were infected at a multiplicity of infection of 10 with transposon mutants, H37Rv, left untreated or treated with staurosporine. Cells were harvested and fixed 4-days postinfection, terminal deoxynucleotidyl transferase dUTP nick end labeling (TUNEL) stained, and analyzed via flow cytometry. Data represent a compilation of four experiments. *Note:* FID = fail to inhibit cell death; STS = staurosporine. * $p < .05$.

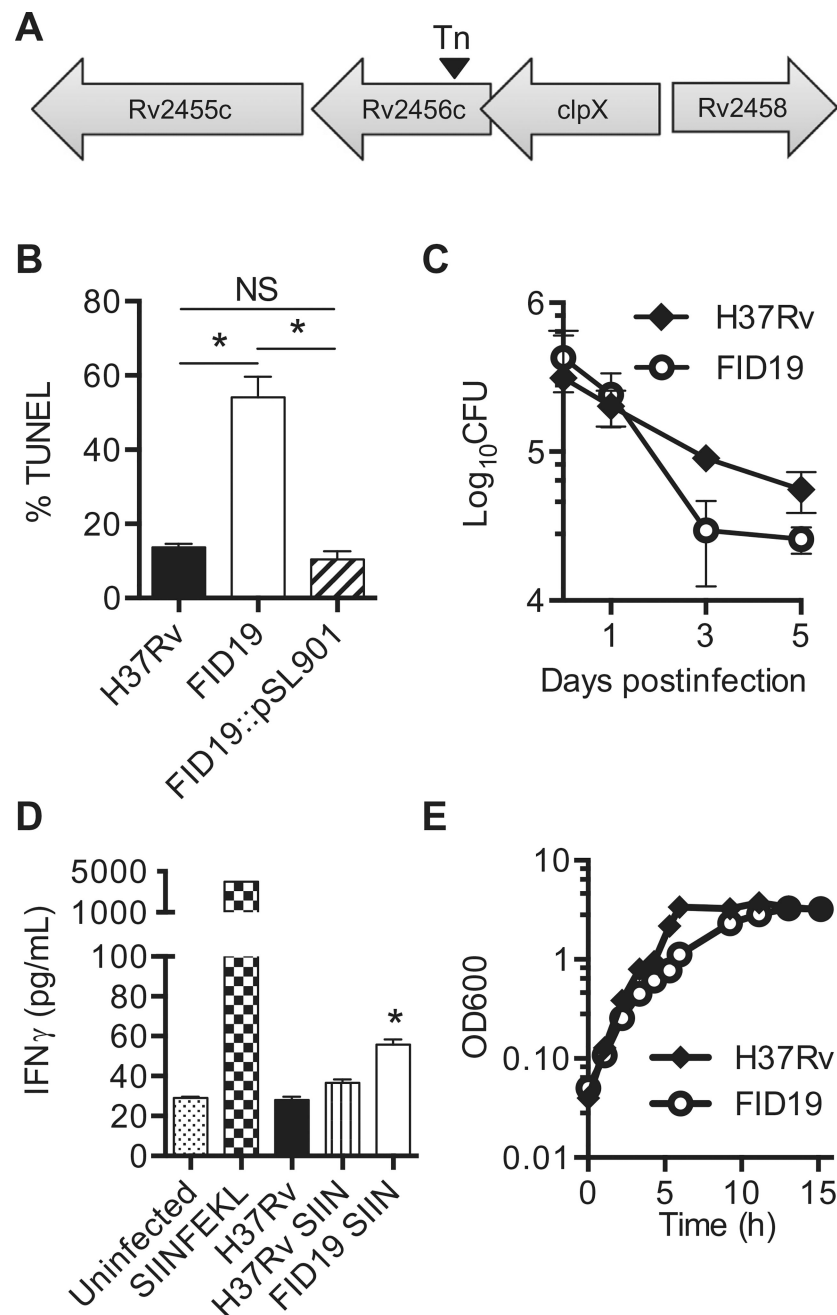


Fig. 2. Rv2456c is important for inhibition of cell death and survival in host cells. (A) Sequencing of the flanking region of the fails to inhibit cell death mutant 19 (FID19) transposon mutant revealed that the insertion occurred between nucleotides 305 and 306 of Rv2456c; (B) THP-1 cells were infected with H37Rv, FID19, or a complementation plasmid (FID19: pSL901) containing *Rv2456c*. Cells were fixed 4-days postinfection, terminal deoxynucleotidyl transferase dUTP nick end labeling (TUNEL) stained, and analyzed via flow cytometry. Data are representative of three separate experiments; (C) THP-1 cells were infected at a multiplicity of infection of 10 with H37Rv or FID19 and plated for colony

forming units at the indicated time points. Data are representative of two independent experiments; (D) bone marrow derived macrophages from C57BL/6 J mice were left untreated, treated with exogenous SIINFEKL as a positive control, or treated with either H37Rv, H37Rv expressing SIINFEKL (SIIN), or FID19 expressing SIIN. After 4 h of treatment or infection, OT-1 CD8⁺ T cells were added to the wells. Supernatant was collected 24-h postaddition of T cells. Secreted interferon- γ (IFN γ) was measured via enzyme-linked immunosorbent assay. Data are representative of three individual experiments; (E) spleens were harvested 3-weeks postretro-orbital intravenous infection with indicated strains and were plated for colony forming units (CFU). Data shown in (E) is a compilation of three independent experiments (2 experiments contained 4 mice/group and the third experiment contained 8 mice/group). * $p < .05$.

Author Manuscript

Author Manuscript

Author Manuscript

Author Manuscript

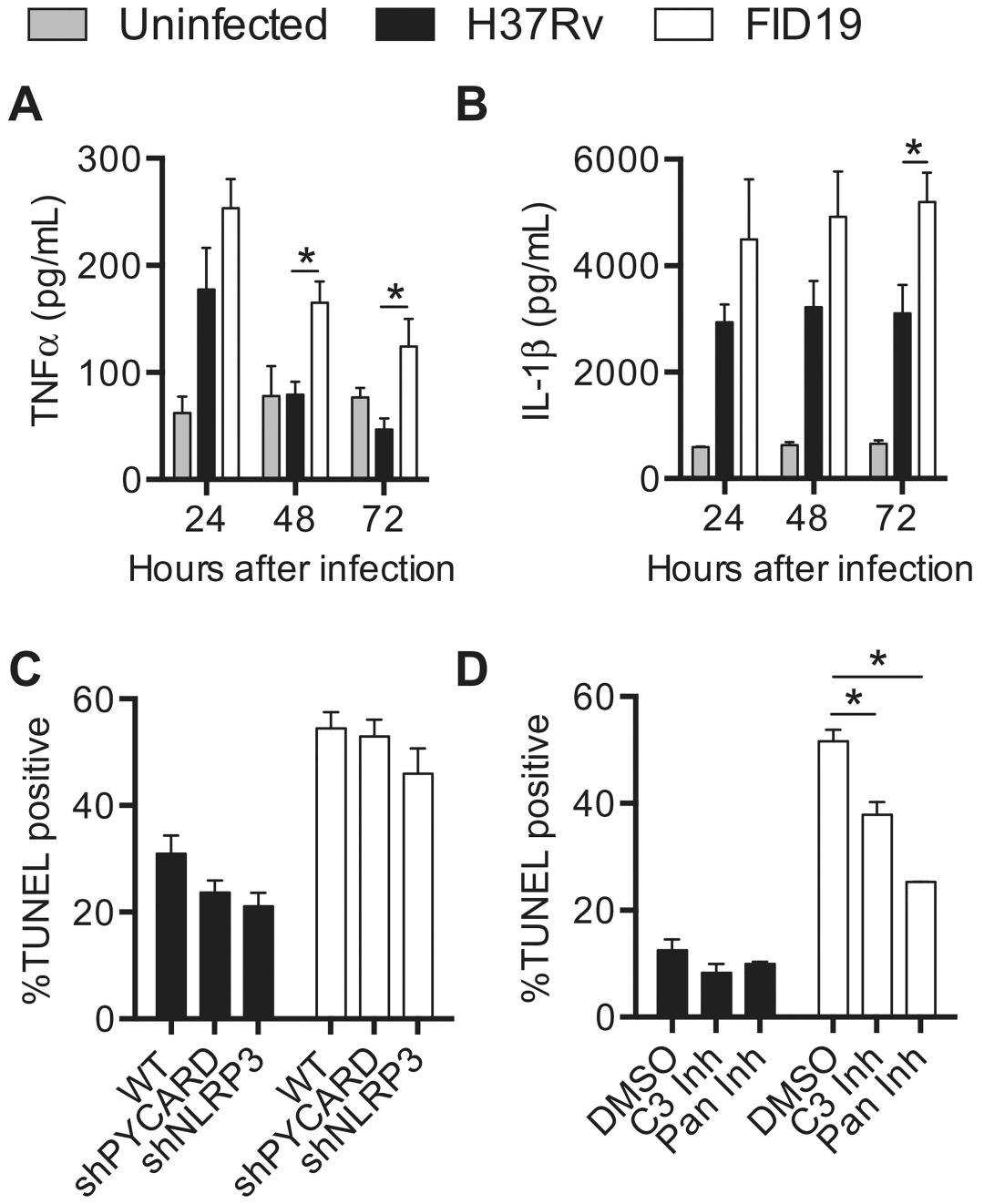


Fig. 3. Fails to inhibit cell death mutant 19-induced cell death through apoptosis. (A, B) THP-1 cells were infected at a multiplicity of infection of 10 and supernatants were collected at indicated time points; (A) tumor necrosis factor- α (TNF α); and (B) interleukin-1 β (IL-1 β) concentrations were assessed via enzyme-linked immunosorbent assay; (C) wild-type or short hairpin RNA knockdown THP-1 cells were infected at a multiplicity of infection of 10 for 3 days with indicated strains, fixed, and terminal deoxynucleotidyl transferase dUTP nick end labeling stained (TUNEL). Data are a compilation of nine experiments; (D) THP-1 cells were infected with indicated strains, treated with dimethyl sulfoxide, 50 μ M caspase 3

inhibitor, or 50 μ M pan-caspase inhibitor. Cells were fixed 3-days postinfection and TUNEL stained. Data are representative of four experiments. * $p < .05$.

Author Manuscript

Author Manuscript

Author Manuscript

Author Manuscript

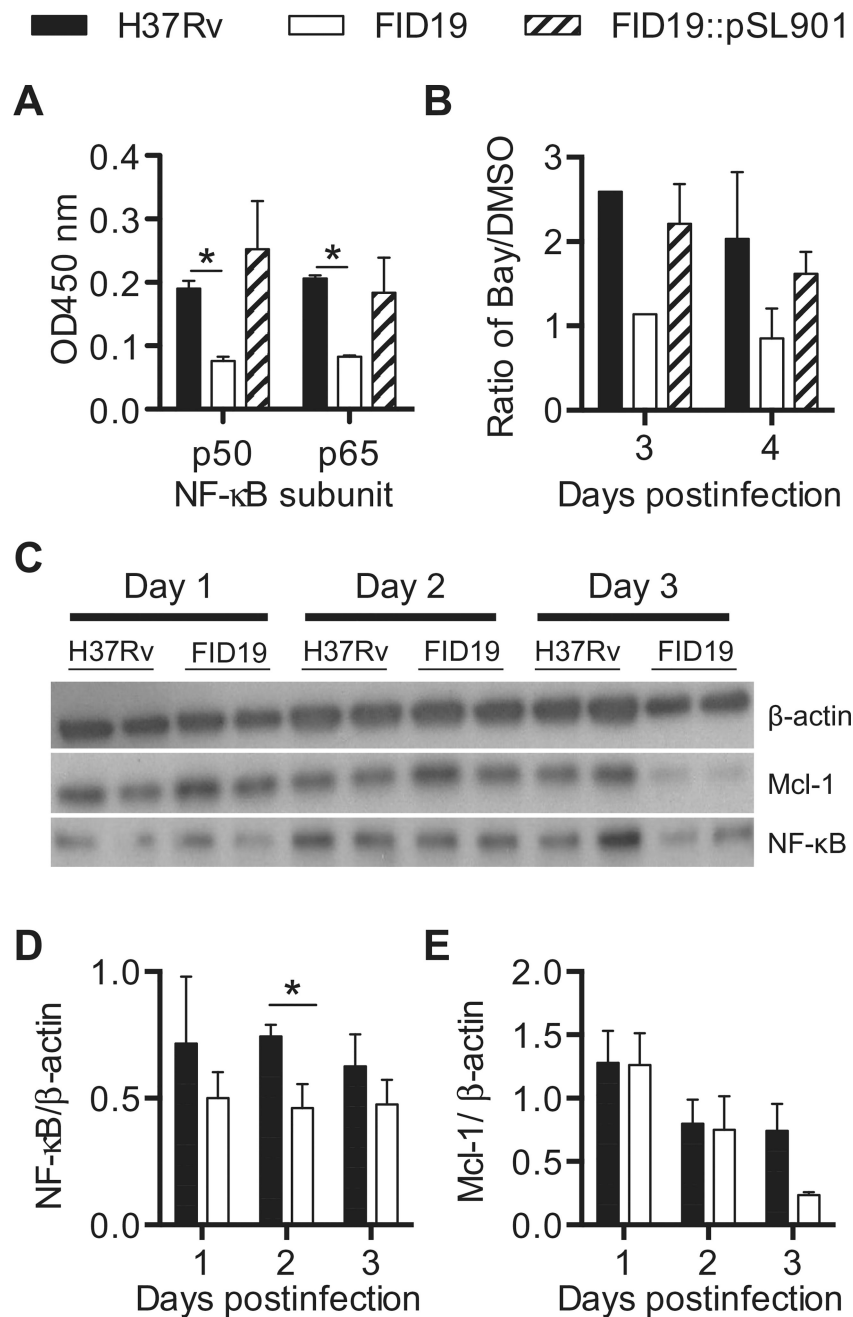


Fig. 4. Nuclear factor- κ B (NF- κ B) activation is reduced during fails to inhibit cell death mutant 19 infection. (A) Nuclear factor- κ B transcription factors p50 and p65 in nuclear extracts of THP-1 cells infected for 2 days with indicated strains were measured via enzyme-linked immunosorbent assay; (B) THP-1 cells were infected with indicated strains and treated with dimethyl sulfoxide or BAY11-7082 for 3- or 4-days postinfection, after which cells were fixed, terminal deoxynucleotidyl transferase dUTP nick end labeling (TUNEL) stained, and analyzed by flow cytometry. Data are presented as terminal deoxynucleotidyl transferase dUTP nick end labeling-positive BAY11-7082-treated cells over dimethyl sulfoxide control

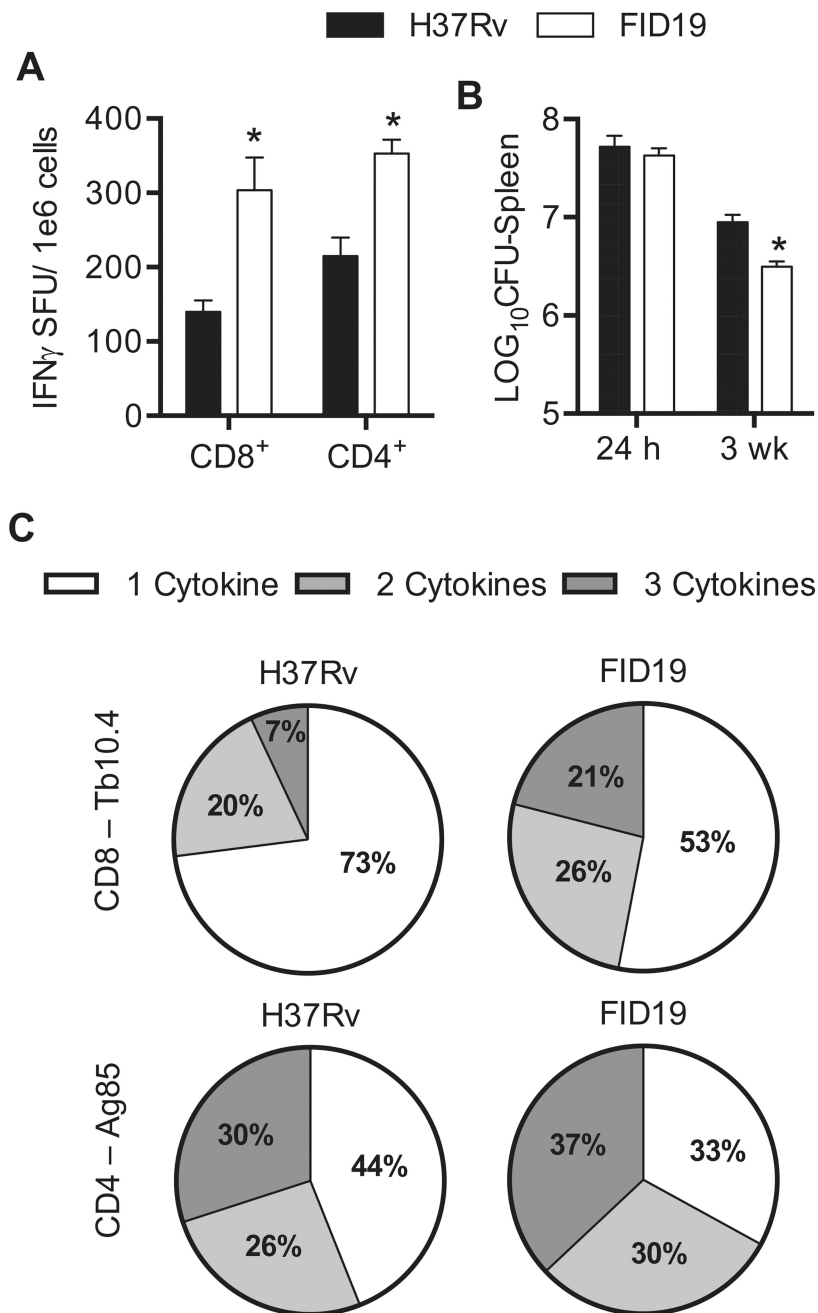
cells and is representative of two experiments; (C) THP-1 cells were infected for the duration of time indicated and protein lysates were acquired and probed for indicated protein; (D, E) densitometry calculations of (C) are shown as a ratio over the β -actin loading control and are a compilation of three separate experiments. * $p < .05$.

Author Manuscript

Author Manuscript

Author Manuscript

Author Manuscript

**Fig. 5.**

Fails to inhibit cell death mutant 19 has enhanced immunogenicity when compared with parental strain H37Rv. (A) C57BL/6 J mice were infected with indicated strain for 3 weeks. Splenocytes were then isolated, stimulated for 24 h with either a CD8⁺-specific antigen (Tb10.4) or a CD4⁺-specific antigen (Ag85) for enzyme-linked immunoSpot analysis. Data are representative of three experiments (2 experiments contained 4 mice/group and the third experiment contained 8 mice/group); (B) splenocytes were isolated, stimulated for 24 h with either a CD8⁺-specific antigen (Tb10.4) or a CD4⁺-specific antigen (Ag85). After the incubation, the cells were stained for CD4⁺ and CD8⁺ surface markers and interleukin-2,

interferon- γ (IFN γ), and tumor necrosis factor- α for intracellular cytokine staining analysis. The data show a representative figure of a standard experiment with four mice/group. *Note:* CFU = colony forming units; SFU = spot forming units. * $p < .05$.

Author Manuscript

Author Manuscript

Author Manuscript

Author Manuscript

Table 1

H37Rv Genes Important for Inhibition of Cell Death Identified in this Study.

FID	Locus Designation	Gene name	Function or product
1	Rv1981c	<i>nrdF1</i>	Involved in the DNA replication pathway
2	Rv1000c		Function unknown
3	Rv0819	<i>mshD</i>	Involved in the fourth step of mycothiol biosynthesis
4	Rv1867		Function unknown, but supposed involvement in lipid degradation
5	Rv2948c	<i>fadD22</i>	Involved in the biosynthesis of phenolic glycolipids
6	Rv1567c		Probable hypothetical membrane protein
7	Rv1436	<i>gap</i>	Involved in the 2nd phase of glycolysis
8	Rv3253c		Possible cationic amino acid transport integral membrane protein
9	Rv0876c		Possible conserved transmembrane protein
10	Rv0110		Probable conserved integral membrane transport protein
11	Rv2019		Unknown, conserved protein
12	Rv1624c		Probable conserved membrane protein, similarity to nuoK
13	Rv1781c	<i>malQ</i>	Probable 4-alpha-glucanotransferase
14	Rv2663		Hypothetical protein
15	Rv2141c		Conserved protein
16	Rv3738c	<i>PPE66</i>	Unknown
17	Rv1704c	<i>cycA</i>	Probable D-serine/alanine/glycine transporter
18	Rv1737c	<i>narK2</i>	Possible nitrate/nitrite transporter
19	Rv2456c		Probable conserved integral membrane transport protein
20	Rv2054		Conserved protein
21	Rv0688		Putative ferredoxin reductase
22	Rv2047c		Conserved hypothetical protein
23	Rv1207	<i>folP2</i>	Dihydropteroate synthase 2

Note. FID = Fail to Inhibit cell Death.